Nanoparticle release from anionic nanocellulose hydrogel matrix

Auvinen, Vili

2022-12

ORIGINAL RESEARCH

Nanoparticle release from anionic nanocellulose hydrogel matrix

Vili-Veli Auvinen [ORCID] **· Patrick Laurén ·**
Boxuan Shen · Jussi Isokuortti · Nikita Durandin ·
Tatu Lajunen · Veikko Linko · Timo Laaksonen

Abstract Nanocellulose hydrogels have been shown to be excellent platforms for sustained delivery of drug molecules. In this study, we examine the suitability of anionic nanocellulose hydrogels for the sustained release of various nanoparticles. Systems releasing nanoparticles could produce applications especially for therapeutic nanocarriers, whose lifetimes in vivo might be limited. Micelles, liposomes and DNA origami nanostructures were incorporated into the nanocellulose hydrogels, and their release rates were measured. Two different hydrogel qualities (with 1% and 2% mass of fiber content) were used for each nanoparticle formulation. We showed that the drug release rates depend on nanoparticle size, shape, and charge. Smaller particles with neutral charge were released faster from 1% hydrogels than from 2% hydrogels. Nanoparticles with cationic labeling were retained in both hydrogels, whereas for the neutral nanoparticles, we were able to determine the cut-off size for released particles for both hydrogels. Rod-shaped DNA origami were released rapidly even though their length was above the cut-off size of spherical particles, indicating that their smaller radial dimension facilitates their fast release. Based on our results, anionic nanocellulose hydrogels are versatile platforms for the sustained release of the chosen model nanoparticles (liposomes, micelles, and DNA

V.-V. Auvinen (✉) · P. Laurén · T. Lajunen · T. Laaksonen
Division of Pharmaceutical Biosciences, Faculty of Pharmacy, University of Helsinki, P.O. Box 56, 00014 Helsinki, Finland
e-mail: vili-veli.auvinen@helsinki.fi

V.-V. Auvinen · J. Isokuortti · N. Durandin · T. Laaksonen
Faculty of Engineering and Natural Sciences, Tampere University, P.O. Box 541, 33014 Tampere, Finland

B. Shen · V. Linko
Biohybrid Materials, Department of Bioproducts and Biosystems, Aalto University School of Chemical Engineering, P.O. Box 16100, 00076 Aalto, Finland

B. Shen
Department of Medical Biochemistry and Biophysics, Karolinska Institutet, 17165 Stockholm, Sweden

T. Lajunen
School of Pharmacy, Faculty of Health Sciences, University of Eastern Finland, Yliopistonranta 1, 70210 Kuopio, Finland

T. Lajunen
Laboratory of Pharmaceutical Technology, Department of Pharmaceutical Science, Tokyo University of Pharmacy and Life Sciences, 1432-1 Hachioji, Tokyo 192-0392, Japan

V. Linko
LIBER Centre of Excellence, Aalto University, P.O. Box 16100, 00076 Aalto, Finland

V. Linko
Institute of Technology, University of Tartu, Nooruse 1, 50411 Tartu, Estonia

origami). Alternatively, for the tightly bound nanoparticles, this could lead to nanoparticle reservoirs within hydrogels, which could act as immobilized drug release systems.

Keywords Nanocellulose · Sustained drug release · DNA origami · Micelles · Liposomes

Introduction

During recent years, many potential nanoparticle drug carriers have emerged for more sophisticated delivery approaches. Micelles, solid lipid nanoparticles, liposomes, nanogels and many other systems have been explored to aid in the delivery and targeting of new compounds, such as biological drugs, that have special challenges and limitations due to their intrinsic properties (Wahlich et al. 2019). For example, sensitivity and stability issues can hinder their efficient administration without encapsulation into a protective carrier. Due to the demanding delivery conditions, more effort should be put into improving compliance, safety, and better control of drug delivery through improved drug administration methods. Most nanoparticle drug delivery approaches utilize repeated injections or infusions with cannulas as their delivery method (Blanco et al. 2015). Therefore, as an alternative method we have investigated the use of a nanohydrogel for an extended delivery of nanoparticles for more steady and controlled drug release rates. The material selected for this study was anionic nanocellulose, also known as anionic nanofibrillated cellulose (ANFC), which is known for its suitability for clinical applications such as wound healing (Koivuniemi et al. 2021). Nanocellulose can be processed to have antimicrobial properties and is generally biocompatible (Norrrahim et al. 2021), and it has been shown to function as an excellent platform for drug release (Paukkonen et al. 2017; Auvinen et al. 2020).

Nanocellulose is a biobased biopolymer in form of a high water content hydrogel which can be processed from the wood pulp of almost any plant material. It forms stable nanofiber networks, each fiber typically 5–20 nm in width, and can be chemically modified through TEMPO [(2,2,6,6-tetramethylpiperidin-1-yl) oxyl] oxidation as a pretreatment method to produce anionic cellulose nanofibers (Gupta et al. 2002; Saito et al. 2006). One environment-friendly manufacturing method for nanocellulose combines low-concentration of cold alkali pretreatment with ultrafine grinding and high-pressure homogenization (Nie et al. 2018). Nanocellulose hydrogels are soft and highly porous materials, and the fiber content of the nanocellulose hydrogel affects the mesh size of the fiber matrix (Kopač et al. 2021). ANFC hydrogel has been demonstrated to perform well with several types of molecules for sustained release, such as small molecules, proteins and both anionic and cationic molecules (Paukkonen et al. 2017) and has been used as a film-like matrix with long-lasting sustained drug release for up to three months (Auvinen et al. 2020). Anionic nanocellulose hydrogels are suitable for formulations that require special processing methods, such as freeze-drying (Koivunotko et al. 2021). Successful release of human VEGF-A and IL-6 proteins were shown after freeze-drying and rehydration of the formulation containing ANFC as the main component (Auvinen et al. 2019). Additionally, nanocellulose hydrogels can be injected subcutaneously, where the injected hydrogel functions as a stable depot (Laurén et al. 2014). In the current study, we examine the release properties of ANFC hydrogel for nanoparticles with varying size, shape, and charge.

Different nanoparticles, varying in size and charge, were prepared for this study: two different types of micelles, four types of liposomes, and DNA origami nanostructures. These nanoparticles represent a small but diverse sample of nanocarriers that have been proposed for use in drug delivery. Micelles were prepared with either Polysorbate 20 (Tween 20) or Poloxamer 407 (Pluronic F127). Tween 20 is a common surfactant and excipient in pharmaceutical formulations used to solubilize low molecular weight compounds or stabilize proteins (Khan et al. 2015), Pluronic F127 micelles have already been shown as successful carriers for drug delivery (Batrakova and Kabanov 2008). Both Tween 20 and Pluronic F127 micelles were labeled with a BODIPY-C12 fluorescent probe that has been used to characterize self-assembling systems (Lisitsyna et al. 2021). Liposomes are the most common and explored nanoparticle delivery systems in pharmaceutical sciences due to their versatility, biocompatibility, and improved targeting and biodistribution of compounds when compared to conventional drug formulations. Currently, there are eight liposomal formulations clinically approved for cancer therapy (Kim and Jeong 2021), and more for other

therapies, such as pain management and age-related macular degeneration (Yuba 2020).

DNA origami nanostructures are self-assembled objects comprising of long single-stranded DNA scaffolds and dozens of short oligonucleotides, so-called staples, which fold the scaffold strand into a pre-designed shape through Watson–Crick base pairing (Dey et al. 2021). Their high homogeneity and excellent addressability allow for a wide variety of chemical modifications at precise locations. This makes them promising candidates for a plethora of applications, including their use as drug delivery vehicles (Seitz et al. 2021). DNA origami carriers can be loaded with various intercalating or groove-binding drugs, such as doxorubicin and methylene blue (Zhao et al. 2012; Zhang et al. 2014; Kollmann et al. 2018; Ijäs et al. 2021). Besides their use as static drug carriers, they can also form dynamic nanodevices which respond to external stimuli, such as selectively releasing/exposing the encapsulated therapeutic molecules (Douglas et al. 2012; Grossi et al. 2017; Ijäs et al. 2019).

The key factors investigated here for ANFC hydrogel formulations were nanoparticle diffusion rates, which parameters affect these rates, and the stability of the nanoparticles in the hydrogel. Our objective was to determine how different sized, shaped and charged particles diffuse out from the ANFC hydrogels, and finally, can the ANFC hydrogels function as a reservoir for nanoparticles.

Materials and methods

Materials

3% anionic nanocellulose hydrogel (research grade, LOT 12,185) was purchased from UPM-Kymmene Oyj, Finland. Dulbecco's Phosphate Buffered Saline, polyethylene glycol (PEG) 8000 for DNA, 1,2-dipalmitoyl-sn-glycero-3-phosphocholine (DPPC), 1,2-distearoyl-sn-glycero-3-phosphoethanolamine-N-[methoxy(polyethylene glycol)-2000] (DSPE-PEG), 1-palmitoyl-2-{12-[(7-nitro-2–1,3-benzoxadiazol-4-yl)amino]dodecanoyl}-sn-glycero-3-[phospho-rac-(1-glycerol)] (16:0–12:0 NBD PG), 1,2-distearoyl-sn-glycero-3-phosphoethanolamine-N-[amino(polyethylene glycol)-2000]-N-(Cyanine 5) (DSPE PEG(2000)-N-Cy5), $MgCl_2$, Tween 20, and

Pluronic F127 were purchased from Merck and used as provided. BODIPY-C12 was synthesized using a previously published method (Levitt et al. 2009). Single-stranded scaffold DNA (p7560) was purchased from Tilibit Nanosystems. Custom staple strands and Atto-488-modified oligonucleotides were purchased from Integrated DNA Technologies (IDT).

Methods

Preparation of the nanoparticles

The micelles were prepared with the molar ratios shown in Table 1. The mixture was stirred for 45 min with a magnetic stirrer to yield a homogenous and clear solution. Chloroform solution of BODIPY-C12 was added while vigorously stirring the micellar solution to yield a total concentration of 5 μM. Upon adding chloroform, the solution turned cloudy. The micellar solution was then stirred for 16 h at room temperature to evaporate the chloroform and yielded again a clear, yellow micellar solution. BODIPY-C12 exhibits absorption and emission maxima around 500 nm and 515 nm, respectively in both chloroform and aqueous micellar solutions.

The liposomes were prepared with compositions shown in Table 1. The lipids were dissolved in chloroform, mixed and the chloroform was evaporated for 45 min in a depressurized rotary evaporator at 64 °C to form a dry lipid film. The film was hydrated by adding 1 ml of deionized water and kept at 64 °C water bath for 20 min, while gently shaken every 5 min. Hydrated lipids were extruded through a porous membrane (50–200 nm) to produce uniform liposomes.

For an exemplary DNA origami, a 24-helix bundle (24HB) was employed. The design was derived from the previously presented work (Ijäs et al. 2021). To attach the Atto-488-modified oligonucleotides (/5ATTO488N/GG GAA AGG AGA AAA AA) to the structure, twelve poly-T overhangs at each side (24 in total) of the original design were replaced by the complementary overhang sequences (5'-TTTTTT CTCCTTTCCC-3'). The self-assembly reaction for the 24HB was carried out using 40 nM p7560 scaffold and 200 nM staple mix in a buffer containing 1 × TAE (40 mM Tris, 19 mM acetic acid, 1 mM EDTA) and 17.5 mM $MgCl_2$ (pH ~ 8.3). The reaction mixture was heated to 65 °C, and assembled by first cooling to

Table 1 Composition and properties of the nanoparticles after preparation and after going through the release testing from the cellulohse hydrogels

	Micelle (7 nm)	Micelle (16 nm)	DNA origami (128×24 nm*)	Liposome (50 nm)	Liposome (80 nm)	Liposome (130 nm)	Cy-5 labeled Liposome (50 nm)
Composition (%)	T-20 BodiPy 99.99 0.01	F-127 BodiPy 99.9 0.1	n.d. (24×Atto488: 1×24HB)	82 DPPC 11 DSPE-PEG 7 NBD	82 DPPC 11 DSPE-PEG 7 NBD	82 DPPC 11 DSPE-PEG 7 NBD	92 DPPC 3 DSPE-PEG 5 Cy-5-PEG
Charge/Z-potential	n.d	n.d	n.d	anionic (−39.9 mV)	anionic (-39.9 mV)	anionic (−39.9 mV)	neutral/cationic (−0,14 mV)
Average size (nm)†	7.48±0.09	16.17±0.69	120.0±3.70	56.53±0.80	78.63±4.41	130.1±3.70	49±2.69
PDI	0.122	0.07	0.117	0.167	0.081	0.097	0.164
D_{S-E} (×10^{-7} cm2/s)	9.78	8.56	5.71	2.74	1.71	1.05	2.74
Hydrogel (w/w %)	1% ANFC / 2% ANFC	1% ANFC / 2% ANFC	1% ANFC / 2% ANFC	1% ANFC / 2% ANFC	1% ANFC / 2% ANFC	1% ANFC / 2% ANFC	1% ANFC / 2% ANFC
D_f (Fitted) (×10^{-9} cm2/s)	88.8 / 135	50.1 / 98.8	192 / 72.0	21.7 / 8.17	8.35 / 1.19	5.51 / 0.288	0.071 / 0.0081
D_{S-E}/D_f	11 / 7	17 / 9	3 / 8	13 / 33	20 / 144	19 / 365	3844 / 33,910
Average size after release (nm)††	6.50±0.45 / 6.87±0.08	16.00±0.68 / 18.92±0.69	114.0±3.60 / 111.1±2.91	67.00±2.18 / 58.41±5.54	82.87±5.33 / 70.54±4.20	114.5±5.30 / 68.05±5.92	62.93±2.52 / 39.92±5.20

* Design parameters. Actual measured measurements in the table

† Diameter at the beginning of the measurement. For DNA origami, length is given instead (nm)

†† Observed average diameter at the end of the measurement, further details in the supplementary data Table ST1

59 °C at a rate of −1 °C/15 min and then to 12 °C at a rate of −0.25 °C/45 min. After thermal annealing, 24HBs were purified from excess staple strands using polyethylene glycol (PEG) precipitation (Stahl et al. 2014) in the presence of 7.5% (w/v) PEG 8000 and 505 mM NaCl. The structures were resuspended in $1\times$TAE and 17.5 mM $MgCl_2$ overnight at 30 °C and then mixed with the Atto-488-modified oligos with a 1:2 ratio. This mixture was then annealed from 40 °C to room temperature at a rate of −0.1 °C/1 min. The fluorescently labeled products were again purified with the above-mentioned PEG precipitation method and resuspended in $1\times$TAE and 17.5 mM $MgCl_2$ at a concentration of ~200 nM.

Preparation of the hydrogel formulations

A total of seven different nanoparticles were used: micelles (diameters 7 nm and 16 nm), neutral liposomes (50, 80, and 130 nm), cationic label modified liposomes (50 nm) and DNA origami (diameter 24 nm, length 120 nm). Each nanoparticle was used in two hydrogel formulations (1% and 2%) which were prepared by mixing the nanoparticle solutions with the hydrogel inside two connected disposable syringes. The contents were pushed from one syringe to the other and vice versa through a connecting rubber tube until homogenous hydrogel was achieved. The measured pH for the anionic nanocellulose was 7.0.

Sustained in vitro release of the nanoparticles

Dulbecco's phosphate buffered saline (DPBS) was selected as the release buffer (2 mL volume, pH 7.4), except for the DNA origami, where Mg-containing TAE-buffer (2 mL volume, pH 8.5) was used to ensure the stability of 24HB in highly anionic environment (Ijäs et al. 2019). The hydrogel formulations were placed inside round plastic wells (Fig. 1 B) with depth of 5 mm and surface area of 38.5 mm^2 and the surface of the hydrogel was evened out with a spatula. The wells were glued on bottom of 24-well plates (Fig. 1 A), and 2 mL of buffer was carefully added on top. The plate was placed in a plate shaker (100 RPM) at 37 °C and protected from light. 100 μL of buffer was collected from each well at each measurement time point and returned to the same well after measuring the amount of release nanoparticles.

Quantification of released nanoparticles

Fluorescent nanoparticle samples collected from the release testing were measured with a Varioskan LUX Multimode microplate reader, and the data was compared to standard curves. The emission/detection wavelengths were as follows: 461 nm/534 nm for NBD, 645 nm/670 nm for Cy-5, 485 nm/520 nm for BODIPY-C12, and 496 nm/521 nm for ATTO-488 – labeled DNA origami.
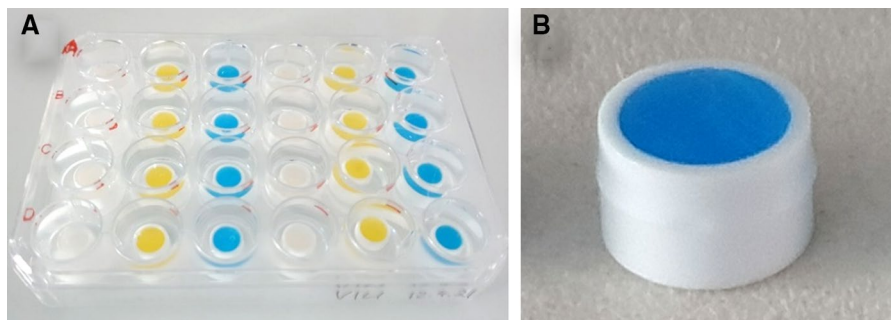

Fig. 1 A The setup for the nanoparticle release experiments, where the white plastic wells filled with nanoparticle-loaded ANFC hydrogels (as shown in B) were glued on a 24-well plate. Anionic nanocellulose formulations carrying DNA ori-gami are light grey in appearance, NBD labeled liposome formulations are yellow, and Cy-5 labeled liposome formulations are blue. Each well has a fresh layer of 2 mL of buffer on top of the wells

Particle size and zeta-potential measurements

The particle size distributions were measured at chosen time points for each nanoparticle with a dynamic light scattering (DLS) technique using a Zetasizer APS (Malvern, USA) instrument. Samples (100 µL) were collected from the same wells used in the release studies at specific time points. The samples were warmed to 37 °C inside the instrument prior to the measurement. Afterwards, the samples were returned to their original sample wells in the 37 °C plate shaker. All the samples were measured in quadruplicate. The values for zeta potential were measured with Zetasizer ZS (Malvern, USA) using disposable capillary cuvettes and diluted as-prepared liposome samples. The particle size distributions were determined by intensity of scattered light and the used dispersant was water for all measurements. A refractive index value of 1.330 was used for the water at 37 °C.

Morphological characterization of the released DNA origami

The DNA origami nanostructures released from the hydrogels were characterized using Tecnai 12 transmission electron microscopy (TEM) manufactured by FEI, USA. Copper TEM grids (FCF400-Cu) were first cleaned with O_2 plasma for 20 s, followed by pipetting of 5 µL of the solution containing released DNA origami on the grid and incubated for 2 min. Then the excess amount of solution was blotted with a piece of filter paper. The sample was immediately stained with 20 µL of 2% uranyl formate for 40 s followed by blotting of the staining solution again with the filter paper. The grid was left to dry for at least 30 min before imaging. Copper TEM grids with both carbon and formvar films (FCF400-Cu) and uranyl formate for negative staining were purchased from Electron Microscopy Sciences.

Rheological measurements

We measured the rheological properties for the 1% and 2% ANFC hydrogels at 37 °C with HAAKE Viscotester iQ Rheometer (Thermo Fisher Scientific, Karlsruhe, Germany). Parallel 35-mm diameter plate-and-plate geometry was used with a 1 mm gap. The hydrogels were warmed to 37 °C before each measurement. Shear viscosity was measured by increasing the shear rate from 0.1 to 1000 1/s during each run. The samples were measured in triplicate and the obtained data was processed with HAAKE RheoWin 4.63 software (Thermo Fisher Scientific).

Results and discussion

Nanoparticle and ANFC characterization

50 nm membrane pores were used to create ~50 nm liposomes, 100 nm pores for ~80 nm liposomes, and 200-nm pores for ~130 nm liposomes. Micelles were considerably smaller (7 nm and 16 nm), while the DNA origami had relatively high aspect ratios (24 nm × 120 nm). Exact sizes are shown in Table 1. 50, 80, and 130 nm liposomes were labeled with NBD. In addition, 50 nm liposomes with cationic Cy-5 label were produced. As the charge is an important property of the liposomes, their zeta-potentials were measured. The NBD-labeled liposomes were anionic as expected for unmodified liposomes, but the Cy-5 labeled liposomes were neutral in charge. This can be associated with the cationic dye group that resides in the hydrophilic part of the modified lipid, whereas the NBD dye is located in the fatty acid chain. Therefore, the charge of the dye is masked in the case of NBD but not in the case of Cy-5. The negligible zeta-potential also indicates that the cationic Cy-5 can almost completely negate the effect of anionic charge at the liposome surface.

As viscosity of the hydrogel is a factor for the release rate, the dynamic viscosity per shear rate was measured for both hydrogels and was lower for the 1% ANFC hydrogel when compared to the 2% hydrogel (Fig. 2). On average, the 2% hydrogel is 2.9 times as viscous as the 1% hydrogel. This is due to higher concentration of fiber in the hydrogel. The dynamic moduli (G′ and G″) of nanocellulose hydrogels are mostly affected by fiber concentration (Mendoza et al., 2018).

Sustained release of nanoparticles

The time scale of nanoparticle release varied from one week to nearly two months depending on the formulation. 100% release was reached only with the smallest particles. No swelling or other morphological changes of the hydrogels were observed during
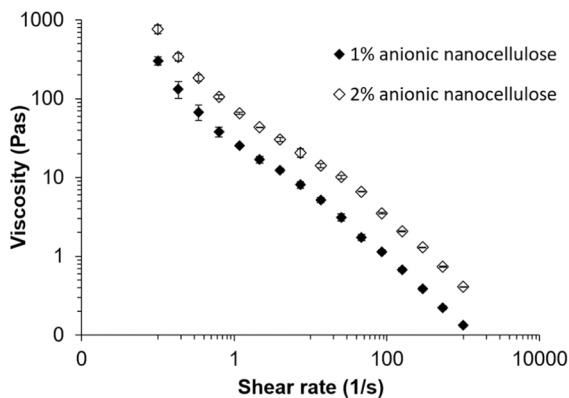
Fig. 2 Viscosity as a function of the shear rate for 1% and 2% anionic nanocellulose hydrogels (logarithmic scale). The stiffer 2% hydrogel is more viscous than the 1% hydrogel

the measurements and the hydrogels stayed stable during the long experiments. The release rates of the smaller nanoparticles in the 1% fiber formulations were faster compared 2% fiber formulations or when compared to the larger particles in either hydrogel (Fig. 3). Rod-like DNA origami demonstrated how the shape affects the release rate; despite their length (120 nm), they were released nearly at the same rate as the small micelles, as the diameter of 24 nm is comparable to that of the micelles (7 and 16 nm) (Fig. 3. During the first hours, cationic labeled and neutral nanoparticles were released rapidly, and afterwards their release rates decreased. Near-complete release was observed for the micelles, DNA origami, and 50-nm anionic liposomes (1% ANFC) during the measurement time windows (4–18 days). However, significantly lower release rates were seen for the larger liposomes and for the 2% hydrogel, which exhibited an incomplete release. The effect of the ANFC concentration was increasingly important for the larger liposomes, and significantly reduced the release of 130-nm liposomes, in particular. This effect can be addressed to the increased viscosity and partly to the mesh size effects. Release of 50-nm liposomes with cationic Cy-5 label was negligible from either type of the hydrogel.

Size distribution changes during the release experiments

To specifically explore the effect of the mesh size and not the viscosity, the size distribution of each

nanoparticle species was monitored throughout the release experiments separately for both hydrogels (1% and 2%). For micelles and DNA origami, no change in size distribution was seen during the release experiments (in neither hydrogel). For the liposome samples, we observed a cut-off effect: The hydrogel samples loaded with liposomes of a larger average size (> 100 nm) first release the smaller particles. Then the mid-sized particles are slowly released. The largest end of the liposome size distribution does not seem to be released practically at all. This affects the observed size distribution of the released nanoparticle population, i.e. the average size appears to be smaller for the released nanoparticles, even though we do not expect the nanoparticles to change shape during the experiments. Depending on the hydrogel fiber content (1% or 2%), the release of liposomes was restricted to certain maximum sizes (Table 1), *i.e.*, ~ 100 nm and ~ 70 nm. For smaller particles, no cut-off effect was observed, indicating facile diffusion in the fiber network. More details of the size distribution data are shown in the supplementary data ST1.

To rule out the possibility of the dissociation of the DNA origami nanostructures, the solution containing the released substances from ANFC hydrogel was imaged with TEM. Numerous released, yet intact, DNA origami were visible in the TEM images after 77 h (Fig. 4A) and 168 h (Fig. 4B), which together with the fluorescent measurements indicated a successful release of nanoparticles.

Mathematical model for the release

To further analyze the obtained release data, we conducted mathematical modeling. The diffusion coefficients (D) for all nanoparticles were calculated based on their release data using an unsteady-state form of Fick's second law of diffusion with early values of time when $0 < M_t/M_\infty < 0.6$ (Siepmann and Siepmann 2012), since the nanoparticles are assumed to behave as simple monolithic solutions (Eq. (1)). The analyzed diffusion coefficients were then compared to estimated diffusion coefficients (D_{S-E}) in plain water derived with the widely known Stokes–Einstein equation (Eq. (2)).

$$\frac{M_t}{M_\infty} = 4\left(\frac{Dt}{\pi L^2}\right)^{\frac{1}{2}} \tag{1}$$

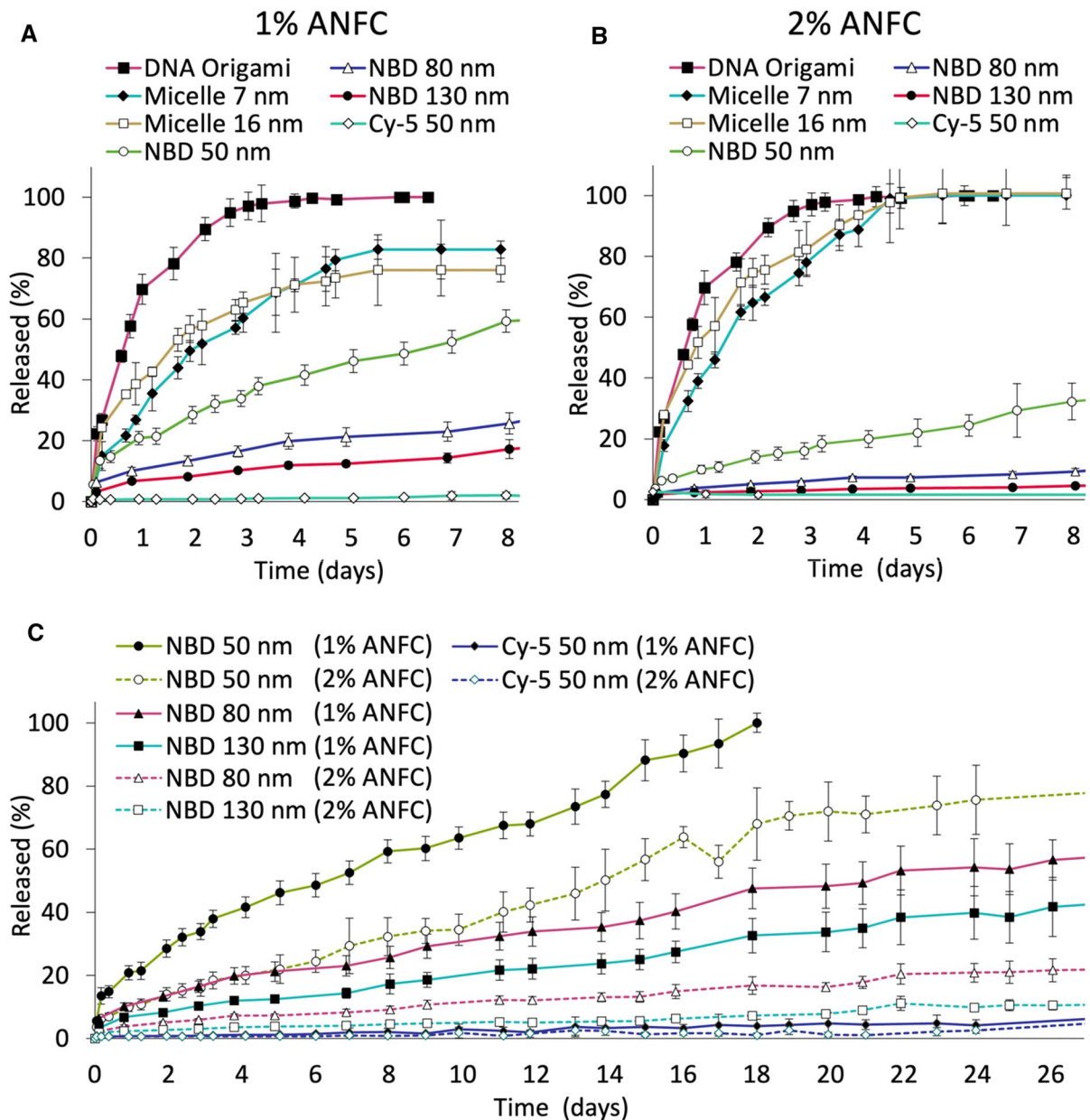**A**

1% ANFC

B

2% ANFC

C

Fig. 3 **A** The release of nanoparticles from 1% anionic nanocellulose (solid lines). **B** The release curves for all nanoparticles from 2% anionic nanocellulose (dashed lines). **C**

Extended-release data of liposomes (NBD and Cy-5 labeled) in 1% and 2% hydrogel formulations (solid and dashed lines, respectively) are shown separately

$$D_{S-E} = \frac{k_B T}{6\pi\eta r} \tag{2}$$

In these equations, M_t/M_∞ is the released fraction of the nanoparticles, D is the diffusion coefficient, t is time, L is the thickness of the hydrogel

layer, T is temperature, η is viscosity, and r is the particle radius.

Finally, the ratio of these two numbers (D_{S-E}/D) is used to get an estimate for the slowing-down of the effective nanoparticle diffusion in the nanocellulose hydrogels (complete data shown in Table 1).
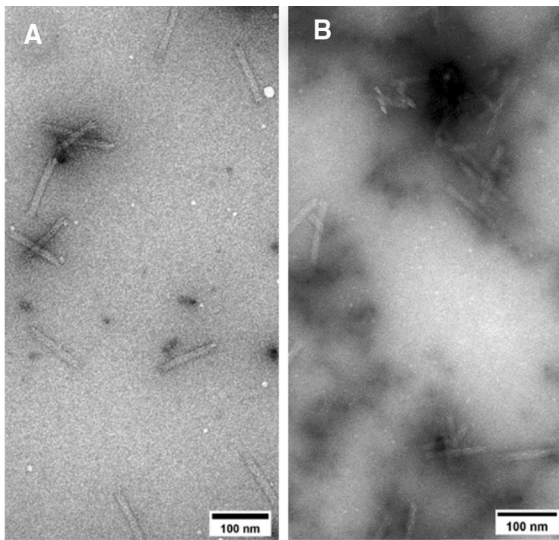
Fig. 4 TEM images showing intact DNA origami released at 77 h **A** and at 168 h **B**

Importantly, the ratio will specifically exclude the direct effect of particle size on *D* and should give an indication of how significant a difference the matrix makes for the release data when compared to plain water. As can be seen in Table 1, the nanocellulose hydrogels decrease the diffusion coefficient of nanoparticles with a factor of ~10 in the case of smaller nanoparticles. However, as the nanoparticle size is increased, the behavior of the two nanocellulose diverge. In the 1% ANFC, the ratio increases moderately to around 25 with larger nanoparticles, indicating some further diffusion barrier for the larger nanoparticles as their average size approaches the mesh size of the hydrogel. In the 2% ANFC, the effect is more pronounced; we observe a significantly reduced diffusion rates in the two larger liposome formulations, which seems to indicate that the effective mesh size of the nanocellulose hydrogel is between 50 and 100 nm. Looking at the other samples, the DNA origami are similar to the smaller nanoparticles in behavior, whereas the cationic labeled liposomes exhibit ratios one or two orders of magnitude higher (>3000). These high values for liposomes with the cationic label can only be explained by strong binding of the liposomes to the nanocellulose network, most likely due to electrostatic interactions. Any phase separations for the nanocellulose hydrogels were not observed.

We have previously determined the release properties of anionic nanocellulose for various model compounds, such as anionic, cationic, neutral, large, and small molecules (Paukkonen et al. 2017). The diffusion coefficients for small molecules varied from 100 to 7000×10^{-9} cm^2/s. Here, the values are consistently lower as the nanoparticles are much larger compared to small molecules. The diffusion coefficient of the smallest nanoparticles, micelles, was close to what has been previously measured for proteins. Here we were able to pinpoint the effects of hydrogel matrix's mesh size (fiber content) on the release rates of possible drug nanocarriers and have further demonstrated that the nanoparticle shape and charge affects the release rate as well. Small nanoparticles with neutral or anionic charge were released from the 1% hydrogels in a similar fashion as could be expected based on simple Stokes–Einstein relation, whereas it took considerably longer time for larger nanoparticles with otherwise similar properties to be released from the 2% hydrogels. The anionic nanocellulose hydrogel barely released any nanoparticles with cationic label. In addition, the larger particles got stuck in the 2% hydrogel as well. The cut-off size appears to be around 100 nm for the 1% hydrogel and 70 nm for the 2% hydrogel. Interestingly, rod-shaped DNA origami were released rapidly despite their considerable length. Based on our results, anionic nanocellulose hydrogel is a suitable platform for the sustained release of the studied nanoparticles with either neutral or anionic surface charge. However, particles with cationic modification get easily stuck in the anionic nanocellulose hydrogel and are barely released. On the other hand, this would be a great advantage for future applications, if nanoscale drug reservoirs are needed as a part of e.g., drug-loaded implants.

Conclusions

Nanocellulose hydrogels are excellent platforms for sustained drug delivery applications, and in this paper, we expanded the release studies to the delivery of nanoparticles. In summary, the obtained in vitro results from the chosen model nanoparticles demonstrate the suitability of the anionic nanocellulose hydrogel for sustained release of various nanoparticles. We were able to determine the cut-off size governed by the fiber density in the hydrogels for

different sized liposomes. In addition, we demonstrated the effect of nanoparticle shape on release profile from ANFC hydrogels by comparing DNA origami nanostructures, micelles and liposomes. We showed that even small liposomes (50 nm) with cationic modification retained much longer in ANFC hydrogel matrix in respect to neutral or negatively charged nanoparticles used in the study. Importantly, all studied hydrogel formulations provided sustained release profiles. This is an important property for applications focusing on sustained release of nanoparticles for therapeutic applications.

References

Auvinen V-V, Merivaara A, Kiiskinen J et al (2019) Effects of nanofibrillated cellulose hydrogels on adipose tissue extract and hepatocellular carcinoma cell spheroids in freeze-drying. Cryobiology 91:137–145. https://doi.org/10.1016/j.cryobiol.2019.09.005

Auvinen V-V, Virtanen J, Merivaara A et al (2020) Modulating sustained drug release from nanocellulose hydrogel by adjusting the inner geometry of implantable capsules. J Drug Deliv Sci Tec 57:101625. https://doi.org/10.1016/j.jddst.2020.101625

Batrakova E, Kabanov A (2008) Pluronic block copolymers: Evolution of drug delivery concept from inert nanocarriers to biological response modifiers. J Control Release 130:98–106. https://doi.org/10.1016/j.jconrel.2008.04.013

Blanco E, Shen H, Ferrari M (2015) Principles of nanoparticle design for overcoming biological barriers to drug delivery. Nat Biotechnol 33:941–951. https://doi.org/10.1038/nbt.3330

Dey S, Fan C, Gothelf K et al (2021) DNA origami. Nat Rev Methods Primers 1:13. https://doi.org/10.1038/s43586-020-00009-8

Douglas SM, Bachelet I, Church GM (2012) A logic-gated nanorobot for targeted transport of molecular payloads. Science 335:831–834. https://doi.org/10.1126/science.1214081

Grossi G, Jepsen MDE, Kjems J, Andersen ES (2017) Control of enzyme reactions by a reconfigurable DNA nanovault. Nat Commun 8:992. https://doi.org/10.1038/s41467-017-01072-8

Gupta P, Vermani K, Garg S (2002) Hydrogels: from controlled release to pH-responsive drug delivery. Drug Discov Today 7:569–579. https://doi.org/10.1016/S1359-6446(02)02255-9

Ijäs H, Hakaste I, Shen B et al (2019) Reconfigurable DNA origami nanocapsule for pH-controlled encapsulation and display of cargo. ACS Nano 13:5959–5967. https://doi.org/10.1021/acsnano.9b01857

Ijäs H, Shen B, Heuer-Jungemann A et al (2021) Unraveling the interaction between doxorubicin and DNA origami nanostructures for customizable chemotherapeutic drug release. Nucleic Acids Res 49:3048–3062 https://doi.org/10.1093/nar/gkab097

Khan TA, Mahler H-C, Kishore RSK (2015) Key interactions of surfactants in therapeutic protein formulations: a review. Eur J Pharm Biopharm 97:60–67. https://doi.org/10.1016/j.ejpb.2015.09.016

Kim E-M, Jeong H-J (2021) Liposomes: biomedical applications. Chonnam Med J 57:27. https://doi.org/10.4068/cmj.2021.57.1.27

Koivuniemi R, Xu Q, Snirvi J et al (2021) Comparison of the therapeutic effects of native and anionic nanofibrillar cellulose hydrogels for full-thickness skin wound

healing. Micro 1:194–214. https://doi.org/10.3390/micro1020015

Koivunotko E, Merivaara A, Niemelä A et al (2021) Molecular insights on successful reconstitution of freeze-dried nanofibrillated cellulose hydrogel. ACS Appl Bio Mater 4:7157–7167. https://doi.org/10.1021/acsabm.1c00739

Kollmann F, Ramakrishnan S, Shen B et al (2018) Superstructure-dependent loading of DNA origami nanostructures with a groove-binding drug. ACS Omega 3:9441–9448. https://doi.org/10.1021/acsomega.8b00934

Kopač T, Krajnc M, Ručigaj A (2021) A mathematical model for pH-responsive ionically crosslinked TEMPO nanocellulose hydrogel design in drug delivery systems. Int J Bio Macromolecules 168:695–707. https://doi.org/10.1016/j.ijbiomac.2020.11.126

Laurén P, Lou Y-R, Raki M et al (2014) Technetium-99m-labeled nanofibrillar cellulose hydrogel for in vivo drug release. Eur J Pharm Sci 65:79–88. https://doi.org/10.1016/j.ejps.2014.09.013

Levitt JA, Kuimova MK, Yahioglu G et al (2009) Membrane-bound molecular rotors measure viscosity in live cells via fluorescence lifetime imaging. J Phys Chem C 113:11634–11642. https://doi.org/10.1021/jp9013493

Lisitsyna E, Efimov A, Depresle C et al (2021) Deciphering multiple critical parameters of polymeric self-assembly by fluorescence spectroscopy of a single molecular rotor BODIPY-C12. Macromolecules 54:655–664. https://doi.org/10.1021/acs.macromol.0c02167

Mendoza L, Gunawardhana T, Batchelor W, Garnier G (2018) Effects of fibre dimension and charge density on nanocellulose gels. J Colloid Interface Sci 525:119–125. https://doi.org/10.1016/j.jcis.2018.04.077

Nie S, Zhang C, Zhang Q et al (2018) Enzymatic and cold alkaline pretreatments of sugarcane bagasse pulp to produce cellulose nanofibrils using a mechanical method. Ind Crop Prod 124:435–441. https://doi.org/10.1016/j.indcrop.2018.08.033

Norrrahim MNF, Nurazzi NM, Jenol MA et al (2021) Emerging development of nanocellulose as an antimicrobial material: an overview. Mater Adv 2:3538–3551. https://doi.org/10.1039/D1MA00116G

Paukkonen H, Kunnari M, Laurén P et al (2017) Nanofibrillar cellulose hydrogels and reconstructed hydrogels as matrices for controlled drug release. Int J Pharm 532:269–280 https://doi.org/10.1016/j.ijpharm.2017.09.002

Saito T, Nishiyama Y, Putaux J-L et al (2006) Homogeneous suspensions of individualized microfibrils from TEMPO-catalyzed oxidation of native cellulose. Biomacromolecules 7:1687–1691. https://doi.org/10.1021/bm060154s

Seitz I, Shaukat A, Nurmi K et al (2021) Prospective cancer therapies using stimuli-responsive DNA nanostructures. Macromol Biosci 21:2100272. https://doi.org/10.1002/mabi.202100272

Siepmann J, Siepmann F (2012) Modeling of diffusion controlled drug delivery. J Control Release 161:351–362. https://doi.org/10.1016/j.jconrel.2011.10.006

Stahl E, Martin TG, Praetorius F, Dietz H (2014) Facile and scalable preparation of pure and dense DNA origami solutions. Angew Chem Int Ed 53:12735–12740. https://doi.org/10.1002/anie.201405991

Wahlich J, Desai A, Greco F et al (2019) Nanomedicines for the delivery of biologics. Pharm 11:210. https://doi.org/10.3390/pharmaceutics11050210

Yuba E (2020) Development of functional liposomes by modification of stimuli-responsive materials and their biomedical applications. J Mat Chem B 8:1093–1107. https://doi.org/10.1039/C9TB02470K

Zhang Q, Jiang Q, Li N et al (2014) DNA origami as an in vivo drug delivery vehicle for cancer therapy. ACS Nano 8:6633–6643. https://doi.org/10.1021/nn502058j

Zhao Y-X, Shaw A, Zeng X et al (2012) DNA origami delivery system for cancer therapy with tunable release properties. ACS Nano 6:8684–8691. https://doi.org/10.1021/nn3022662

Publisher's Note Springer Nature remains neutral with regard to jurisdictional claims in published maps and institutional affiliations.